

This article was downloaded by:

On: 30 January 2011

Access details: *Access Details: Free Access*

Publisher *Taylor & Francis*

Informa Ltd Registered in England and Wales Registered Number: 1072954 Registered office: Mortimer House, 37-41 Mortimer Street, London W1T 3JH, UK



Separation & Purification Reviews

Publication details, including instructions for authors and subscription information:

<http://www.informaworld.com/smpp/title~content=t713597294>

ELECTROKINETIC ANALYZERS

Paul Todd^a; John Pellegrino^b

^a Department of Chemical Engineering, University of Colorado, Boulder, CO, U.S.A. ^b Physical and Chemical Properties Division, National Institute of Standards and Technology, Boulder, CO, U.S.A.

Online publication date: 02 July 2000

To cite this Article Todd, Paul and Pellegrino, John(2000) 'ELECTROKINETIC ANALYZERS', *Separation & Purification Reviews*, 29: 1, 149 — 169

To link to this Article: DOI: 10.1081/SPM-100100007

URL: <http://dx.doi.org/10.1081/SPM-100100007>

PLEASE SCROLL DOWN FOR ARTICLE

Full terms and conditions of use: <http://www.informaworld.com/terms-and-conditions-of-access.pdf>

This article may be used for research, teaching and private study purposes. Any substantial or systematic reproduction, re-distribution, re-selling, loan or sub-licensing, systematic supply or distribution in any form to anyone is expressly forbidden.

The publisher does not give any warranty express or implied or make any representation that the contents will be complete or accurate or up to date. The accuracy of any instructions, formulae and drug doses should be independently verified with primary sources. The publisher shall not be liable for any loss, actions, claims, proceedings, demand or costs or damages whatsoever or howsoever caused arising directly or indirectly in connection with or arising out of the use of this material.

ELECTROKINETIC ANALYZERS

Paul Todd¹ and John Pellegrino²

¹Department of Chemical Engineering,
University of Colorado, Campus Box 424,
Boulder, CO 80309-0424

²Physical and Chemical Properties Division,
National Institute of Standards and Technology,
325 Broadway, Boulder, CO 80303

ABSTRACT

Electrokinetic analysis is a family of techniques for estimating the charge on solid surfaces, macroscopic particles, colloidal species, and macromolecular aggregates. Charges on surfaces are critical to the behavior of colloids, coatings, films, fibers, and many other materials in a variety of application areas. In addition to estimating the charge, electrokinetic analysis provides the means for measuring how the surrounding medium and imposed electric fields interact with extended flat surfaces, channels, pores, particles, and molecular aggregates to produce motion. Such motion has found wide use as a means for separating complex mixtures into their components. This section will present how measurements are made, some theoretical underpinnings, and examples of the instrumentation used for making measurements.

The submitted manuscript has been authored by a contractor of the U.S. Government. Accordingly, the U.S. Government retains a non-exclusive, royalty-free license to publish or reproduce the published form of this contribution, or allow others to do so, for U.S. Government purposes.

THE ELECTROKINETIC PHENOMENA

The four principal electrokinetic processes of interest (Table I) are electrophoresis (motion of a particle in an electric field), sedimentation potential (the creation of a potential by particle motion, the reverse of electrophoresis), electroosmosis (the induction of flow at a charged surface by an electric field, the opposite of electrophoresis), and streaming potential (the creation of a potential by fluid flow, the reverse of electroosmosis).

These phenomena are all reflections of the interaction of dissolved charges (ions) with a surface carrying a “fixed” surface charge density leading to a *zeta potential* (defined below) at the plane of hydrodynamic shear. Electrokinetic phenomena (Fig. 1) always occur, and their relative magnitudes determine the practicality of an electrokinetic measurement. Their interrelatedness can be appreciated in terms of the reciprocal transport relationships derived from the work of Onsager. In Onsager’s analysis the total material flow (J) and current (I) result from contributions from both the gradients in total mechanical driving force (ΔF) and electric field (ΔE). The reciprocal nature requires that if flows are induced then, alternatively, both types of forces can be measured. Therefore, the effect of the zeta potential is manifested in either of two ways. Either motion is created by the application of an electric field or an electric field arises as a result of motion. The constant material property that links motion to field is *electrophoretic mobility*, defined as the velocity per unit field

$$\mu_e = v/E. \quad (1)$$

In most cases μ_e is directly proportional to the zeta potential, which is, in turn directly proportional to the surface charge density σ_e . Thus, electrokinetic analyzers may be used for the estimation of surface charge densities. The details of the relationships specific to each case are summarized in later sections.

Table I. Principal Electrokinetic Processes

Technique	What is Measured	What Moves	What Causes Movement
Electrophoresis	Velocity	particles move	applied electric field
Electroosmosis	Velocity	liquid moves in capillary	applied electric field
Streaming Potential	Potential	liquid moves	pressure gradient
Sedimentation Potential	Potential	particles move	gravity = $g\Delta r$

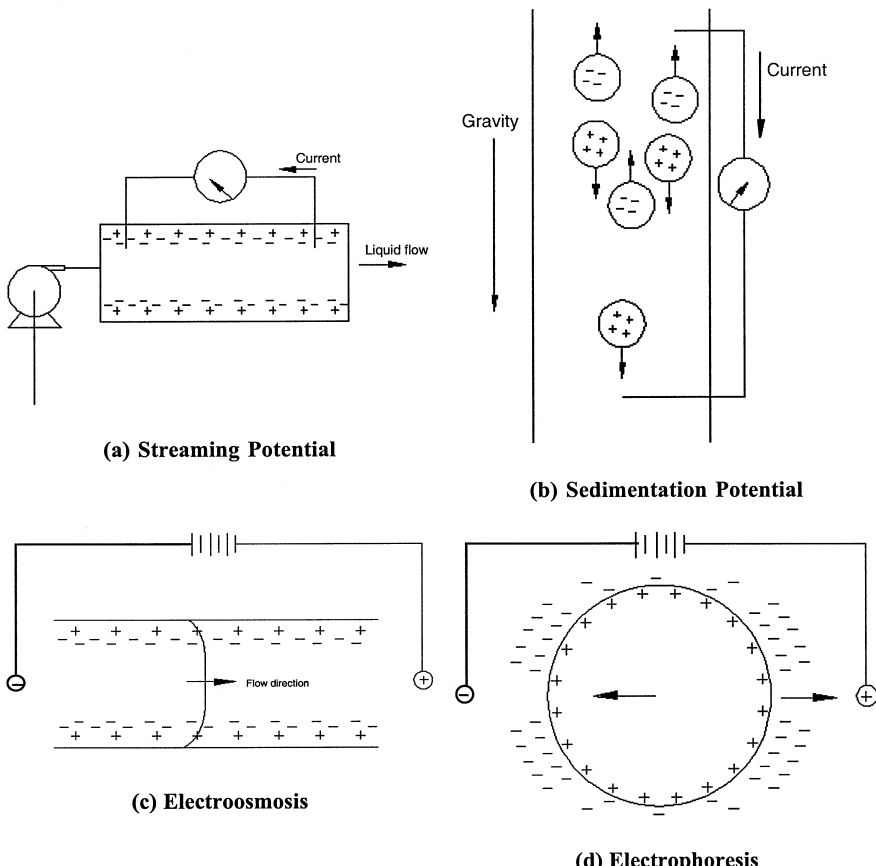


Figure 1. The four electrokinetic processes: (a) streaming potential, (b) sedimentation potential, (c) electroosmosis and (d) electrophoresis (Copyright American Chemical Society, by permission).

THE ELECTRIC DOUBLE LAYER

Fig. 2 is a schematic diagram of the electrokinetic boundary layers characteristic of a solid surface containing immobilized electrical charges in contact with an aqueous solution of mobile ions that screen these charges. The electric double layer is generally viewed as consisting of two layers: an immobile layer of ions opposite in sign to that of the surface and a diffuse layer—a cloud of hydrated ions that transitions from the significant excess of counterion at the fixed charge layer to a balance of cations and anions in the bulk solution. This double layer surrounds

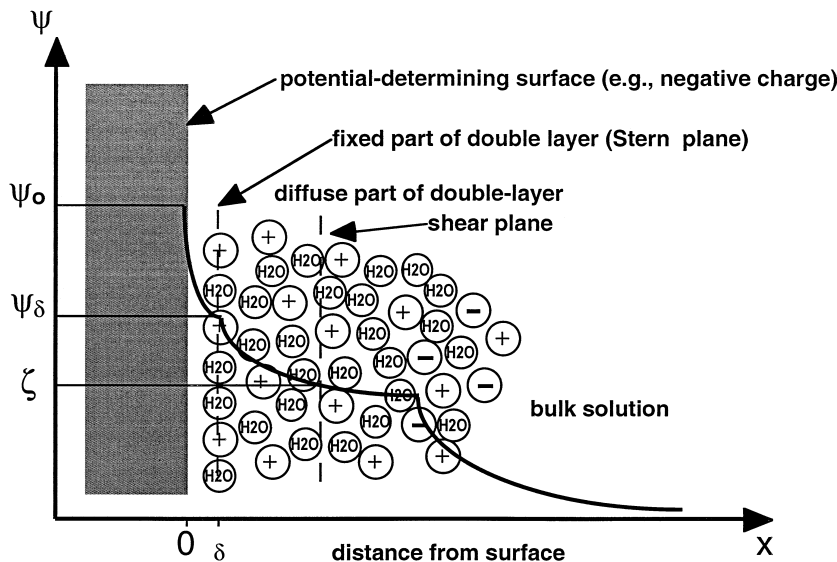


Figure 2. Schematic diagram of the electric double layer model of a non-conducting surface, including colloidal particles, in contact with an electrolyte solution (the surface is assumed to have net negative charge in this schematic). δ represents the distance of closest approach for a mobile counterion to the surface charge. The Ψ axis is depicted with the absolute value of the potential. Ψ_0 is the surface potential, Ψ_δ is the Stern potential, and ζ is the zeta potential. Note that the shear plane is usually assumed to be in the diffuse layer. The actual shape of the potential drop from the surface ($\Psi = \Psi_0$) to the bulk solution ($\Psi = 0$) can be very variable.

all charged macromolecules and particles in solution and plays a role in several properties of significance in chemical analysis and processing including (but not limited to): precipitation, flocculation, electrophoresis, colloid stability, phase partitioning, and sorption.

The place of electrostatic forces (and therefore electrokinetic measurements) in particle (or macromolecule) interactions with each other and macroscopic surfaces can be understood in terms of the total potential energy of interaction V_T as it varies with separation distance x . In the simplest case, $V_T(x)$ is the sum of the electrostatic repulsion curve $V_R(x)$ and the attractive potential curve $V_A(x)$. At very close distances there is a deep minimum ($V_T \ll 0$) which represents a stable configuration for the two surfaces. At farther separations a repulsive energy barrier may exist, but still farther apart a small secondary minimum ($V_T < 0$) may also exist that represents another stable association between the surfaces. The shape of the $V_T(x)$ curve will dramatically depend on the longer range electrostatic interactions between the surfaces. For example, if particles with negative

(see Fig. 2) surfaces approach one another in an electrolyte solution, the attracting forces responsible for $V_A(x)$, such as London and van der Waals forces, are opposed by the repulsion of like charges in the double layer. If the surface charge can be reduced or screened by dissolved ions then a closer approach is possible, allowing the attractive nature of London and van der Waals forces to be more effective. Particles or surfaces attached to each other at this “secondary minimum” are still some 5–50 nm apart.

In Fig. 2 the surface itself is considered to have a net excess of fixed negative charges. These cannot be removed, but they can be neutralized, one at a time, by the inward diffusion of “counterions” (ions of charge opposite to the fixed ions) causing a *fixed layer* where electrostatic attraction balances back-diffusion and mobile ion repulsive forces; this is the Stern layer. Its thickness (δ) is less than 1 nm. At greater distances from the fixed-charge surface, diffusion (energy = kT) is comparable to the residual potential energy, and the result is a *diffuse layer* in which ion diffusion is weakly affected by the electrostatic potential $\psi(x)$, which eventually falls to 0 defining the outer boundary of the double layer. The *shear plane* is assumed to be in the diffuse layer, close to the boundary between the fixed and the diffuse layers. The “thickness” of the diffuse layer (x_{DL}) is often expressed as the *Debye length* (also called the ion atmosphere radius), which depends on the concentration of dissolved ions and is the reciprocal of the *Debye-Hückel parameter* (κ):

$$1/x_{DL} = \kappa = [(e^{2\sum} n_{i0} z_i^2) / (\epsilon \epsilon_0 kT)]^{1/2} \quad (2a)$$

where the summation is over all ions (i) in solution, and n_{i0} = number of ions of type i in the bulk solution, z_i = charge on ion i, e = electron charge (1.602×10^{-19} C), ϵ = dielectric constant (= 80 for pure water and most dilute solutions), and ϵ_0 = permittivity of free space (8.854×10^{-12} C 2 ·J $^{-1}$ ·m $^{-1}$), k = Boltzmann constant J·K $^{-1}$, T = temperature, K. For aqueous solutions at 25 °C and converting the ion concentrations into molar terms yields

$$\kappa = 2.32 \times 10^9 (\sum c_i z_i^2)^{1/2} \quad (2b)$$

where c_i is in mol·dm $^{-3}$ and κ is in m $^{-1}$.

There are various theories describing the electric double layer. The Gouy-Chapman (G-C) theory, one of the first, assumes a) a flat, impenetratable surface, b) ions in solution are point charges, c) the surface charge and potential are uniformly distributed upon the surface, and d) the solvent properties (including dielectric constant) are independent of distance from the surface. All of these assumptions are questionable, and more complex theories have evolved, but nonetheless the G-C theory provides an often-used tool for obtaining quantitative information about the double layer. For the case of two types of ions of equal and opposite charge z , the G-C theory states that the electrical potential decreases

with distance x according to

$$\frac{d\Psi}{dx} = -(2kT/ze)\kappa \sinh(ze\Psi/(2kT)). \quad (3)$$

For symmetrical electrolytes the surface charge density ($C \cdot m^{-2}$) is

$$\sigma_0 = [8n_0\epsilon\epsilon_0 kT]^{1/2} \sinh(ze\Psi_0/(2kT)). \quad (4)$$

For the simplified case of 1-1 electrolytes and low surface potential Ψ_0 (~ 25 mV) then a solution for the potential from Eq. (3) is given by

$$\Psi(x) = \Psi_0 \exp(-\kappa x). \quad (5)$$

This relationship illustrates the effect of ionic strength on the double layer—as the ionic strength increases, $\kappa\kappa$ (Eq. (2b)) increases and the distance from the surface at which $\Psi(x)$ is $1/e$ ($\sim 1/2.72$) of its surface value decreases.

For convenience, Eq. (2b) has been plotted for different electrolyte types, 1:1, 1:2, 2:1, 1:3, etc. cation valence:anion valence, in Fig. 3. Thus the effects of the addition of indifferent electrolytes (those that do not specifically adsorb) are

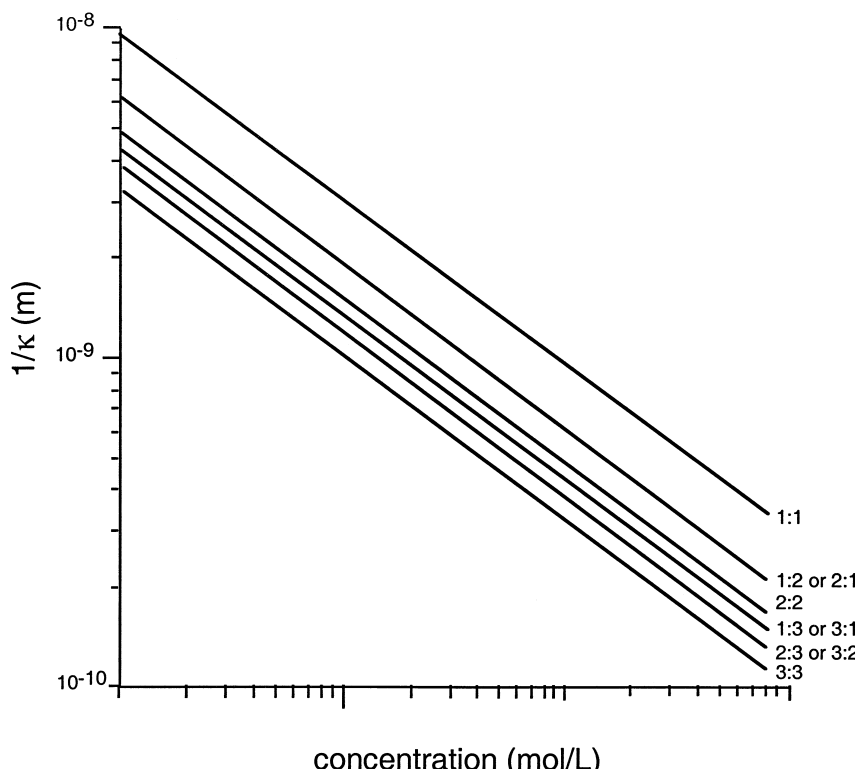


Figure 3. The effect of electrolyte molarity and valence on the Debye length ($1/\kappa$) in water at 27 °C and $\epsilon = 80$. (Copyright American Chemical Society, by permission.)

to reduce the double-layer thickness (often referred to as charge screening) and promote closer approach of surfaces and increased adhesion (and possibly decreased electrophoretic or electroosmotic mobility).

In Fig. 2 the vertical dashed line showing the position of the shear plane intersects the potential curve at the *zeta potential*, ζ ?(mV). This is the potential that is measured in an electrokinetic analysis and is the potential that determines the electrophoretic mobility (μ_e , typically expressed in units $\mu\text{m}\cdot\text{s}^{-1}/(\text{V}\cdot\text{cm}^{-1})$) of particles and colloids as given by the Smoluchowski equation.

$$\mu_e = \epsilon\epsilon_0\zeta/\eta \quad (6)$$

where η = viscosity ($\text{g}\cdot\text{cm}^{-1}\cdot\text{s}^{-1}$).

ELECTROKINETIC ANALYSIS OF SURFACES AND COATINGS

General Principles

Streaming Potential

The relationship between the streaming potential and the zeta potential can be understood by considering a stream of electrolyte being forced to flow between two parallel plates (Fig. 1a), separated by distance $2B$, due to an applied pressure drop ΔP . The velocity at any given position x is given by

$$v = \Delta P B^2 / 2\eta L [1 - (x/B)^2], \quad (7)$$

where x is the variable distance between planes with $x = 0$ at the centerline between the two plates, and L is the chamber length. In the electrolyte that lies within one Debye length of the shear plane, where $x = B - (1/\kappa)$ the flow velocity is

$$v = \Delta P B / \kappa \eta L. \quad (8)$$

Therefore some of the ions in the double layer are carried by the flowing solution, and a streaming current I_s is established that is determined by the wetted perimeter ($2BY$), the surface charge density at the shear plane σ_e , and the velocity at the Debye length (Eq. 8):

$$I_s = 2BY\sigma_e \Delta P / \kappa \eta L. \quad (9)$$

The resulting net movement of ions results in a streaming potential E_s , which can be measured in millivolts by a voltmeter and that is directly related to the zeta potential. At steady state the streaming potential produces a conduction current that just balances the streaming current and depends on the resistance presented by the channel, and will in fact depend on the surface conductance. The zeta potential can be determined by applying Ohm's law and the above relationships

$$\zeta = E_s \eta L / A R \epsilon \epsilon_0 \Delta P \quad (10)$$

where A = cross-sectional area of the chamber perpendicular to the direction of flow, and R = ohmic resistance of electrolyte (which may also include the surface conductance) in the chamber. This is the "Helmholtz-Smoluchowski" relationship.

Streaming potential can also be used to determine the zeta potentials of irregularly shaped objects that can be immobilized in a flow chamber. It is assumed that the electrokinetic surface area is predominantly that of the sample material, which is packed in a cylindrical chamber, that the test material is non-conductive, and that the surrounding flowing electrolyte, at >1 mM with conductivity k , carries most of the current. Then the Helmholtz-Smoluchowski Eq. (10) can be modified to give

$$\zeta = E_s \eta k / \epsilon \epsilon_0 \Delta P. \quad (11)$$

Electroosmosis

In an open system, in which fluid flow in the direction of the applied electric field is possible, the net negative charge on a wall results in plug-type electroosmotic flow (EEO) that enhances total fluid transport according to the Helmholtz relationship integrated over the double layer at the chamber wall

$$v = \epsilon \epsilon_0 \zeta E / \eta = \mu_{eo} E \quad (12)$$

In a closed system, such as is used in many practical cases, flow at the walls must be balanced by return flow in the opposite direction. Therefore, within a closed cylindrical tube, as used in electrophoresis, for example, the flow profile is a parabola

$$v = (\epsilon \epsilon_0 \zeta E / \eta) (r^2 / R^2 - 1/2). \quad (13)$$

Thus, if the electroosmotic mobility μ_{eo} is high (of the order $1 \mu\text{m}\cdot\text{s}^{-1}/(\text{V}\cdot\text{cm}^{-1})$), then sample zones of particles or solutes, if present, will be distorted into parabolas. An additive parabolic pattern is superimposed if there is a radial temperature gradient that causes a viscosity gradient. High temperature in the center of the chamber results in low viscosity and higher velocity. In stationary-sample applications, however, open-ended systems are normally used, and the simple velocity given by Eq. (12) is equal to the fluid flux, which can be measured by accumulating fluid that flows through the test chamber as described below.

Instrumentation

Instrumentation for Streaming Potential Measurements

Streaming potential measurements of films (or flat surfaces) are typically implemented by the application of Eq. (10) to a channel formed by two parallel pieces (for example, the sample plates in Fig. 4a) of the subject material. A thin

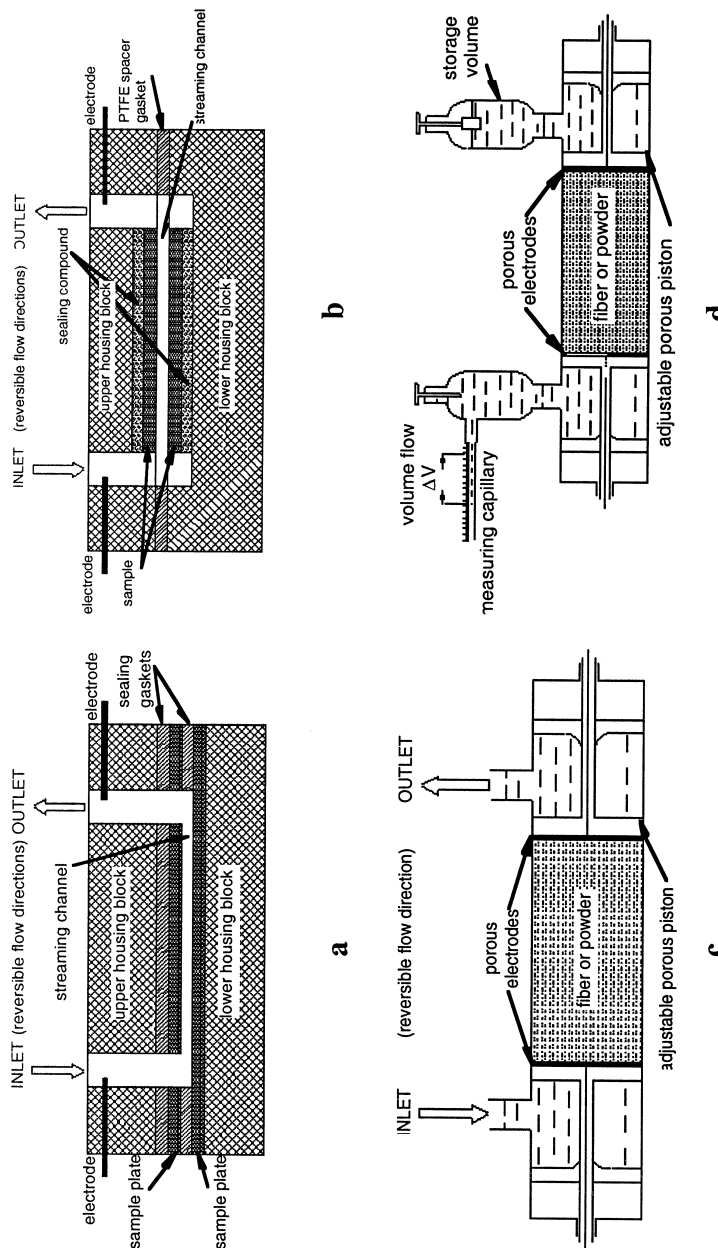


Figure 4. Chambers for streaming potential and electroosmosis measurement. (a) For measuring zeta potential of solid surfaces of test plates.

(b) For measuring zeta potential of flat, porous continuous media between plates. (c) For measuring zeta potential of irregular solids, fibers, granules and the like. (d) For measuring electroosmotic flow rate to determine zeta potentials of chamber walls or packing material in the test chamber. (Diagrams courtesy of Brookhaven Instruments Corp.)

layer of electrolyte solution is passed between the plates using a known pressure drop ΔP , and the resulting streaming potential is measured, as shown schematically in Fig. 4a. Alternatively, the space between the plates can be occupied by a felt, sponge, or continuous porous medium whose zeta potential is to be determined, as in Fig. 4b. When the zeta potential of a bed of irregularly shaped objects, including fibers, powders, granules, or microporous filter is to be determined, they are mounted in a cylindrical cell (between flow-through electrodes), as shown in Fig. 4c, and Eq. (11) is used to calculate the zeta potential from the measured streaming potential as electrolyte is pumped through the bed (or pores) under pressure ΔP .

Instrumentation for Electroosmosis Measurements

In the closed-system method, the velocity parabola due to an applied electric field is measured in a thin rectangular or cylindrical chamber. The intrinsic electrophoretic velocity of a marker particle or solute must be subtracted before calculating the wall's zeta potential from Eq. (13). This method is further discussed under microscopic electrophoresis, below.

In the open-chamber method, wall zeta potential or the zeta potential of a packing material in an electroosmosis cell can be determined by the application of a current that will drive fluid through the chamber as shown in Fig. 4d. The mass of collected fluid is used to determine the volumetric flow rate, from which v and hence ζ are determined.

Examples of Measurements

It is often desirable to know conditions (pH, ionic strength) under which a surface has zero net charge and/or its highest net charge in an electrolyte solution, since these conditions determine the adhesive properties of the material. Fig. 5 is an example of a streaming potential measurement for viscose fibers. It indicates that the fibers are neutral at pH ~ 2.3 , their isoelectric point (IEP). The absolute accuracy of zeta potential measurements can be quite variable (typically on the order of $\pm 1\text{--}4$ mV); therefore the uncertainty in IEP determinations may be on the order of ± 0.4 pH units. But the qualitative and quantitative differences among materials measured in a proximal sequence are typically repeatable.

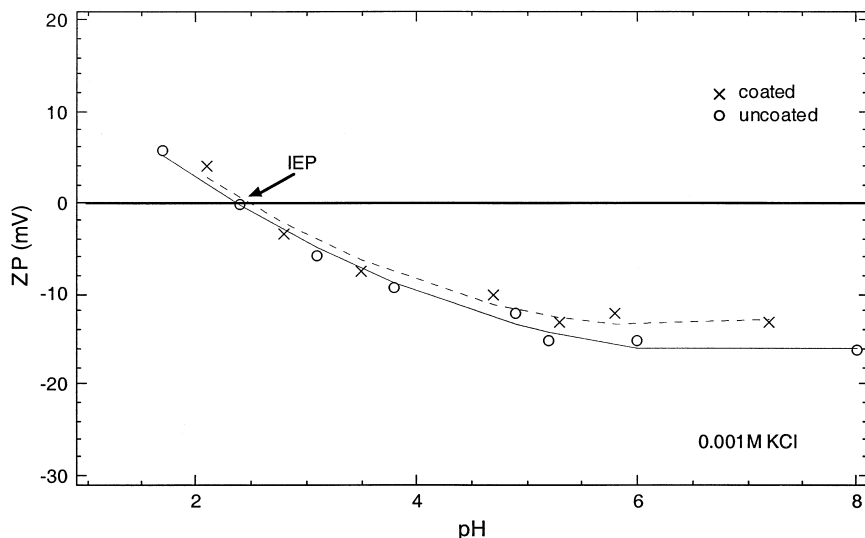


Figure 5. Comparison of the pH dependence of the zeta potentials (ZP) of two samples of viscose fibers. IEP = isoelectric pH. (Copyright American Chemical Society, by permission).

ELECTROKINETIC ANALYSIS OF PARTICLES AND COLLOIDS

There are two principal methods for determining the zeta potential of suspended particles and colloids: *analytical electrophoresis* (optical or acoustical particle motion analysis) or *preparative electrophoresis* (particle separation in an electric field). There are several instrumental methods corresponding to each of these, and these are enumerated in the following paragraphs.

Analytical Electrophoresis

Electrophoresis is the motion of particles (molecules, fine particles, and whole biological cells) in an electric field. The particle electrophoretic mobility μ_e (as defined earlier) is a characteristic of individual particles and can be used as a basis of colloid stability or separation and purification. The surface charge density of suspended particles prevents their coagulation and leads to stability of lyophobic colloids (not having a strong affinity for the dispersing phase). This stability determines the success of paints and coatings, pulp and paper, sewage and fer-

mentation, and numerous other materials and processes. The surface charge also leads to motion when such particles are suspended in an electric field. The particle surface's zeta potential (in a given ionic environment) will interact with the applied field in a manner similar to that outlined previously for electroosmosis. For particles that are large (such as cells and organelles) when compared with the double layer thickness ($\kappa r \gg 1$, r = particle radius), then the electrophoretic velocity is given by Eq. (12). For small particles ($\kappa r \ll 1$), such as molecules, whose radius is similar to that of a dissolved ion (Debye-Hückel particles), then the electrophoretic velocity is given by

$$v = (2\epsilon\epsilon_0\zeta E)/(3\eta) = \mu_e E. \quad (14)$$

The mobilities (v/E) will be intermediate between Eq. (12) or (14) at moderate ionic strengths (0.01–0.2 equiv./L) and for colloidal-sized particles. In this case the literature contains corrections for retardation caused by counterions and charged particles and for relaxation caused by distortion of the diffuse double layer. In general, because of the uncertainties in calculating the zeta potential, electrokinetic measurements on particles are simply quoted as the unambiguously measured mobility.

Sedimentation Potential

Sedimentation potential is another means of measuring the zeta potential of suspended charged particles (refer to Fig. 1). As implied in the opening equations of this section, if a particle is caused to move by the acceleration of gravity (upward or downward), the strength ($V \cdot \text{cm}^{-1}$) of the electric field generated is

$$E = 4\zeta\epsilon\epsilon_0(\rho - \rho_0)g/(3\eta\kappa) \quad (15)$$

where ρ is the particle density, ρ_0 is the fluid density, and g is the gravitational constant. This potential is also known as "counterstreaming potential" and as the "Dorn effect." This potential could be as great as 20 mV, which should be easily measured and is comparable to a typical particle zeta potential. Instrumentation for sedimentation potential measurements is not popularly used, but the same principle is applied to concentrated suspensions in which the acceleration is acoustic rather than gravitational.

Preparative Electrophoresis

Different methods of electrokinetic analysis by electrophoretic particle separation exist. While well over a dozen such methods can be used for particle preparative separations, the following also have been used as electrokinetic analyzers: free-zone electrophoresis, density gradient electrophoresis, and free-flow electrophoresis.

Analytical electrophoresis in a gel matrix is very popular, because convection is suppressed; however, most particles do not migrate in most gels. Capillary zone electrophoresis, a powerful, high-resolution analytical tool, depends on processes at the micrometer scale and is not applicable to particle electrophoresis ($>1\text{ }\mu\text{m}$). Therefore particle electrophoresis must be performed in free fluid, so great care must be taken to prevent free and forced convection and particle sedimentation. The two most frequently used free fluid methods are zone electrophoresis in a density gradient and free-flow (or continuous flow) electrophoresis. Temperature control is generally imposed on all free-fluid electrophoresis systems as a means of suppressing thermal convection and avoiding viscosity gradients. When the particle density exceeds the fluid density by more than 0.03 g/cm^3 , free electrophoresis in a density gradient is dominated by sedimentation, while separation by free flow electrophoresis is less so.

Resolution varies among preparative electrophoresis methods. Any method that divides the outflow into j equal fractions will have an intrinsic minimum *geometrical coefficient of variation* (CV) of $1/j$. Uniform particle populations have intrinsic CV's around 0.05, or 5% of their mean mobility, so every collected fraction should migrate at least 20 fractions to take full advantage of the resolution offered by free preparative electrophoresis methods. The practical limit of the total number of fractions that can be collected from a given separation device, NSU (number of separation units) is usually specified by the equipment design. CV is not a simple reciprocal of NSU, as the measured electrophoretic standard deviation accounts for physical distortion of separand zones and other stochastic factors in addition to the finite size of collected fractions. So, as a rule. $\text{CV} > 1/\text{NSU}$.

Instrumentation - Analytical Electrophoresis

Analytical electrophoresis instruments fall into two broad categories: microscopic electrophoresis - consisting of directly observing individual particle motion and deriving particle velocities or optical or acoustic techniques - in which particle motion is discerned from the analysis of light scattering signals or the electrical response of a particle suspension to monochromatic acoustic energy. In all cases, electroosmosis, discussed above, plays a role in the accuracy and/or interpretation of analytical electrokinetic data on particles and colloids.

Microscopic Electrophoresis

Manual observation and recording of electrophoretic mobilities is achieved by applying an electric field to a small cylindrical or rectangular chamber under a microscope objective. The general principle can be understood from Fig. 6a. Elec-

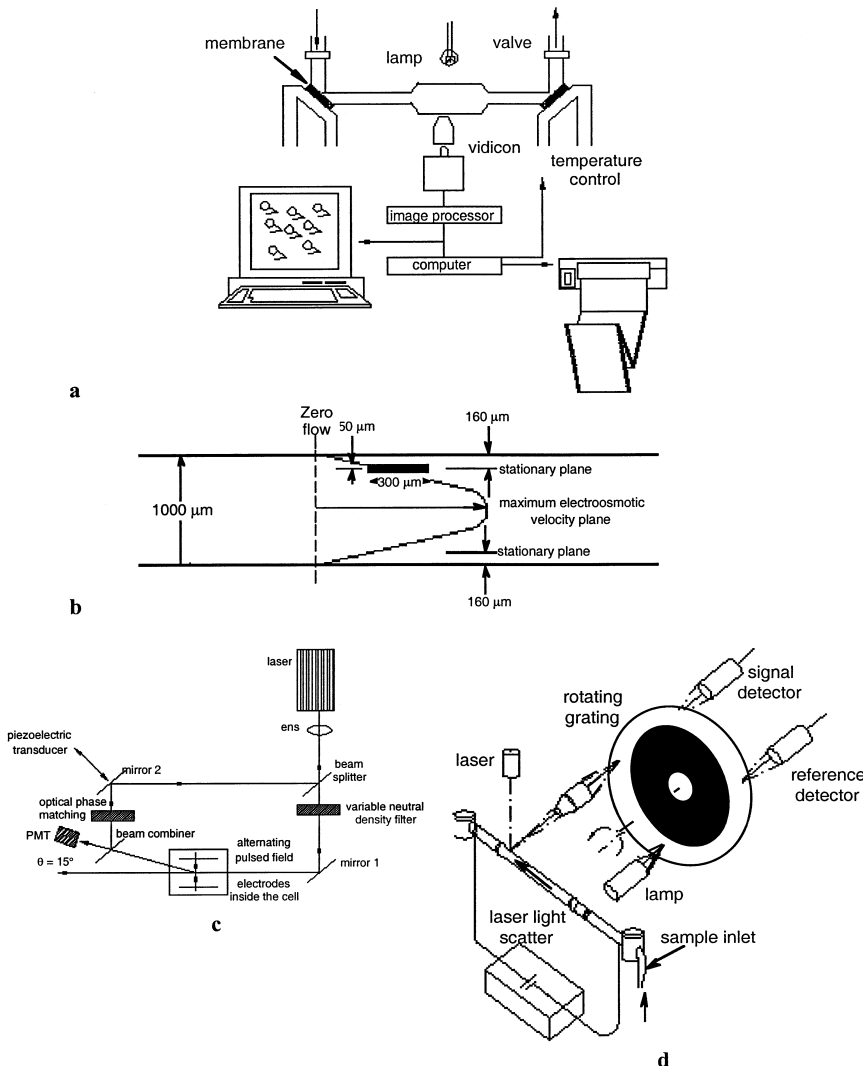


Figure 6. Methods of particle analytical electrophoresis. (a) Schematic diagram of microscopic electrophoresis chamber with computerized motion analysis (Copyright CRC Press, by permission). (b) Electroosmotic flow profile in a closed microscopic electrophoresis chamber (Courtesy of D. Fairhurst, Brookhaven Instruments Corporation). (c) Schematic diagram of a laser Doppler velocimetry system (Courtesy of D. Fairhurst, Brookhaven Instruments Corporation). (d) Schematic diagram of laser frequency-modulation apparatus (Copyright W. DeGruyter AG, by permission).

troosmosis due to the charged walls of the chamber results in flow toward the cathode along the walls and, if the chamber is closed, return flow toward the anode at the center of the chamber. Partway between the cathodic and reverse flows, the flow of electrolyte solution is 0, and this region is called the stationary plane (Fig. 6b, where all electrophoretic motion is due to particle electrophoresis. The operator clocks the motion of about 100 particles, one at a time, between grid lines on an ocular reticle and determines particle velocities at the stationary plane by one of two methods: making all observations at the two stationary planes only or collecting velocities as a function of chamber depth and fitting the best parabola.

Automated versions of microscopic electrophoresis have been developed, and particle speeds are determined by a motion analysis algorithm tied directly to a video camera output (Fig. 6a). The algorithm is capable of calculating mobilities automatically and reporting mobility histograms.

Laser Doppler Velocimetry and Fringe Anemometry

Laser Doppler velocimetry enjoys widespread use in the study of fluid motion in general. It was adapted to electrokinetic analysis in the 1970's. The frequency of incident electromagnetic wavefronts meeting a stationary illuminated particle is given by

$$\nu = c/\lambda,$$

where c = speed of light in vacuum, and λ = wavelength. But if the particle is moving with velocity vector v_i in the direction of wave propagation, the frequency of wavefronts incident, and therefore scattered, becomes

$$\nu_p = (c - v_i)/\lambda.$$

The difference between the incident and scattered frequencies is the well-known Doppler shift. If the angle between incident and scattered light paths is Θ and the magnitude of the particle's velocity is v_i (see Fig. 6c), then this frequency difference is

$$\nu_D = \nu_p - \nu = (2nv_i/\lambda)\sin(\Theta/2), \quad (16)$$

where n = refractive index of the suspending medium in which the wave is propagated. For typical particle electrophoretic velocities, $\nu_D = 10\text{--}100$ Hz, while ν_p for visible laser light is around 10^{15} Hz. This tiny frequency shift can be detected only by optical heterodyning, in which wavefronts scattered from the moving particle are recombined with wavefronts from a stationary source, giving the well-known beat, or heterodyne frequency such as that heard when two mandolin strings are not too closely tuned. The heterodyne frequency can be seen as a modulated intensity output from a square-law photodetector such as a photomultiplier

tube. The components of a light-scattering electrophoretic analyzer are shown in Fig. 6c.

In another form of laser light-scattering electrophoresis a fully automated device analyzes the frequency of modulation of light scattered though a rotating grating from moving cells in comparison with the modulation frequency of light from a stationary source, as shown schematically in Fig. 6d. The resulting power spectrum, produced by a fast Fourier transform, is used to calculate an electrophoretic mobility histogram from corresponding absolute velocities and the automatically measured electric field using the simple relationship

$$\mu_e = fL/ME, \quad (17)$$

where f = frequency shift due to electrophoresis, M = optical magnification, and L = periodicity of the grating. An example of electrophoretic mobility measurements with this technique is shown in Fig. 8b.

Acoustophoretic Analysis

The principle of acoustophoretic analysis was introduced by P. Debye long before it was implemented. Its lack of volume and concentration constraints is its greatest advantage. The method is also tolerant of a wide range of ionic strengths and pH values. A sonic transducer introduces acoustic energy into a volume of any size located between two sensing electrodes. The sound-induced motion of the charged particles in suspension causes an AC current to flow between the reversible electrodes. The phase relationship between the resulting current and the input sonic wave is then used for the calculation of ζ .

Analysis by Preparative Electrophoresis Methods

There are two very broad categories of preparative particle electrophoresis methods, static column methods and flowing methods. While these methods are applicable to electrokinetic measurements they are not as popular as light scattering methods.

Free-Zone Electrophoresis

Free-zone electrophoresis or horizontal column electrophoresis has been performed in rotating tubes of 1–3 mm inner diameter. The small diameter minimizes convection distance and facilitates heat rejection while rotation counteracts all three gravity-dependent processes: convection, zone sedimentation, and parti-

cle sedimentation. The concept is illustrated in Fig. 7a, which shows that the total vertical velocity vector oscillates as a sample zone moves in the electric field, so that spiral motion results. In small-bore tubes with closed ends, scrupulous care must be taken to suppress electroosmotic flow by using a nearly neutral, high-viscosity coating, and rapid heat rejection and/or low current density is necessary to minimize radial thermal gradients.

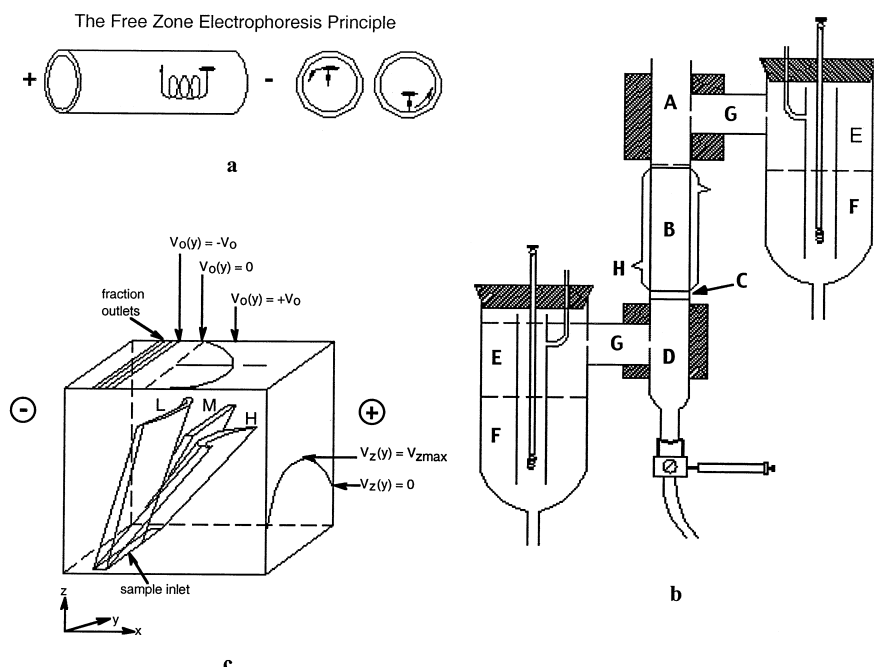


Figure 7. Methods of preparative electrophoresis applicable to the measurement of particle electrophoretic mobility (a) Free zone electrophoresis showing trajectory followed by a particle in a rotating tube. (b) Density gradient electrophoresis column labeled to indicate the location of various solutions at the start: A. Top buffer, B. Migration zone with density gradient, C. Sample to be separated, D. Dense solution at bottom of column, E. Top solution, F. Electrode solution in which electrodes are immersed, G. Gel plug or membrane, H. Thermostated jacket. (c) Diagram (not to scale) of an upward-flowing free flow electrophoresis chamber. A coordinate system with (0,0,0) at the lower front left corner is shown. Sample stream is shown as a slit (circular sample streams are commonly used). Anodal migration of low, medium, and high (L,M,H) mobility separands results in crescent-shaped bands due to Poiseuille retardation of particles near the walls (where $v_z(y)$ is low) in the case of high-mobility and electroosmotic flow near the walls (where $v_o(y)$ is high) in the case of low mobility. These two parabolic distortions balance in the case of medium-mobility separands. (Copyright American Chemical Society, by permission.)

In a free-zone electrophoresis system with a 20 cm long x 3 mm diameter rotating tube (with no electroosmotic flow), a practical minimum collection volume of 0.05 mL from a total of 1.5 mL gives NSU = 30, and the results of optical scanning of the electrophoresis tube during a run (shown in Fig. 8a) results in a CV = 5%. A single batch separation requires about 20 min, and the efficient heat transfer allows experiments in up to 0.15 M (isotonic) salt solution. The main

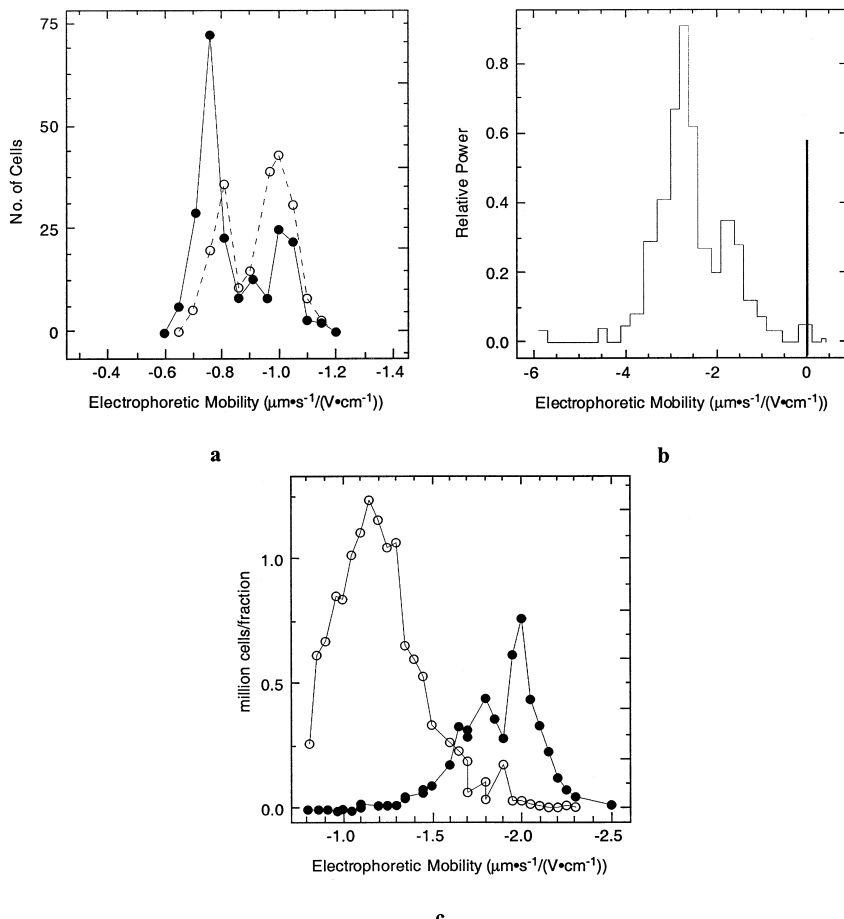


Figure 8. Examples of electrophoretic mobility measurements by (a) Automated microscopic electrophoresis (Copyright CRC Press, by permission) and (b) Laser frequency-modulation electrophoresis (Copyright American Chemical Society, by permission) (c) Free flow electrophoresis. Particles in all examples were mixed populations of biological cells.

sources of inconvenience are the preparation of the electrophoresis tube with a low electroosmotic-flow coating and the meticulous task of loading the sample.

Density Gradient Electrophoresis

Density gradient electrophoresis has been used for protein and virus separation and has been shown to separate particles on the basis of electrophoretic mobility. A typical column is shown in Fig. 7b. The use of a density gradient counteracts (within calculable limits) all three effects of gravity: particle sedimentation, thermal convection and zone, or droplet, sedimentation. The migration rates of particles in a density gradient are, however, quantitatively different from those observed under typical analytical electrophoresis conditions, because (1) the sedimentation component of the velocity vector increases as the density of the suspending fluid decreases upward, (2) the viscosity of the suspending solution decreases with increasing height, and (3) the conductivity of the suspending electrolyte increases, consistent with the viscosity reduction.

If the anode is at the top and the particles are negatively charged, the instantaneous migration velocity of a particle (undergoing upward electrophoresis) in a vertical density gradient may be described by

$$v(x) = [\mu_e E(x)] - [2r^2 g(\rho - \rho_o(x))/9\eta(x)], \quad (18)$$

where, in typical situations of interest, inertial and diffusion terms are neglected. In Eq. (18), x is defined as the vertical distance from the starting zone, μ_e is the anodic electrophoretic mobility, $E(x)$ is the electric field strength, usually determined from

$$E(x) = I/(A k(x)), \quad (19)$$

in which I is the constant applied current, k is the conductivity of the gradient solution, and A is the cross-sectional area of the gradient column. The second term of Eq. (18) represents the sedimentation velocity for spheres of radius r . The x -dependent variables are explicitly indicated in Eqs. (18) and (19).

Explicit expressions have been established for the x -dependent variables to allow integration of Eq. (18) to yield the distance of migration up the column as a function of time of application of the electric field without using fitted parameters; therefore, μ_e can be determined absolutely and from this the zeta potential. In cases of a narrow particle density distribution the gradient may be tailored so that the particles are close to neutral buoyancy over an appreciable distance of the column.

In a typical column of 30 mL, 0.05 mL fractions could be collected, giving $NSU = 600$, but more typically, $CV = 5\%$, which seems to be the lower limit for any preparative electrophoresis method. The principal inconvenience of this

method is the forming of the density gradient, however, this is a routine procedure in some professions, especially including experimental biochemistry. Density gradients typically used range from $0.67 \text{ mg} \cdot \text{cm}^{-3} \cdot \text{cm}^{-1}$ for long (10 cm) columns to $20 \text{ mg} \cdot \text{cm}^{-3} \cdot \text{cm}^{-1}$ for short (1.5 cm) columns.

Free-Flow Electrophoresis

A continuous free-flow electrophoresis system is shown diagrammatically in Fig. 7c, where the thickness of the chamber is shown highly exaggerated for clarity. Several investigators have constructed mathematical models of free-flow electrophoresis. The main ingredients of such a model include the following variables: electrophoretic migration of separands, Poiseuille flow of pumped carrier buffer, electroosmosis at the front and back chamber walls, horizontal and vertical thermal gradients, conductivity gradients, diffusion, sample input configuration, and fraction collection system. Fig. 7c indicates the path followed by three categories of separands, low, medium and high mobility, and indicates the effects of Poiseuille flow and electroosmosis when sample is injected at the bottom, electrophoresis is to the right, and fractions are collected at the top. A coordinate system is shown in which the z axis is the direction of pumped fluid (buffer) flow, the y axis is the chamber thickness, and the x axis is the chamber width and direction of migration of separands in the applied, horizontal electric field. Separands will arrive at the outlet end of the chamber distributed in nested crescents in which high-mobility separand particles nearest the front and back walls migrate the farthest, as indicated in Fig. 7c.

Typical dimensions of available free-flow electrophoresis chambers is $x_m = 6\text{--}15 \text{ cm}$, $y_m = 0.03\text{--}0.15 \text{ cm}$, and $z_m = 22\text{--}110 \text{ cm}$, where the subscript m designates distance to the opposite wall from the origin. The motion of a particle through such a chamber is complex. The migration distance x is the sum of electrophoretic migration and electroosmotic flow

$$x = \mu_e E \tau(y) + v_{eo}(y) \tau(y), \quad (20)$$

where τ = residence time of the separand in the cell. But $\tau(y)$ and $v_{eo}(y)$ are explicit functions of y. Approximate relationships can be derived for the overall motion of a separand particle in free flow electrophoresis by substituting explicit geometrical functions into Eq. (20) to give

$$x(y) = \{2EZ_m(\mu_e - \mu_{eo}/2)\}/\{3V_{zav}[1 - (y-b)^2/b^2]\}. \quad (21)$$

This relationships states that the direction of the parabola depends on the relative magnitudes of the separand mobility and the electroosmotic mobility (μ_{eo}) of the chamber wall, where the geometrical variables are defined in Fig. 7c. In the examples illustrated in Fig. 7(c), high-mobility separands (H) migrate far-

thest to the right near the chamber walls, while low (L) or zero-mobility separands move farthest to the left near the chamber walls.

Practical chamber thicknesses are limited to about 0.5 mm. Free-flow electrophoresis units have been constructed with 20 to 197 outlets, so at the current state of the art, $NSU = 197$. The corresponding theoretical CV is 0.5%, which has never been achieved. From the data in Fig. 8c a measured CV for a mixture of fixed erythrocyte cells could be determined, giving $CV = 7.1\%$. Some aspects of free flow electrophoresis make it convenient: no density gradient, continuous sample collection, and potential for real-time optical monitoring. A few commercial versions of free-flow electrophoresis equipment exist.

SUGGESTED READING LIST

J. Bauer, ed., "Cell Electrophoresis," CRC Press, Inc. Boca Raton. 1994.

W. Schütt and H. Klinkmann, eds., "Cell Electrophoresis," Walter deGruyter, Berlin. 1985.

P. G. Righetti, C. J. van Oss, and J. Vanderhoff, eds., "Electrokinetic Separation Methods," Elsevier/North-Holland Biomedical Press, Amsterdam, 1979

D. Fairhurst and V. Ribitsch, in "Particle Size Distribution II," T. Provder, ed., ACS Symposium Series No. 472, American Chemical Society, Washington, 1991, pp. 337-353.

R. Hidalgo-Alvarez, *Adv. Coll. Int. Sci.* 34, 217-341, (1991).

R. J. Hunter, in "Zeta Potential in Colloid Science, Principles and Applications" R. H. Ottewill and R. L. Rowell, eds., Academic Press, New York. 1981, p. 125

R. J. Hunter, "Introduction to Modern Colloid Science," Oxford University Press:, Oxford. 1996.

R. W. O'Brien and L. W. White, *J. Chem. Soc. Faraday II*, 74, 1607-1626, (1978).

S.R. Rudge and P. Todd, in "Protein Purification from Molecular Mechanisms to Large-Scale Processes" M.R. Ladisch, R.C. Willson, C-d. C. Painton, and S.E. Builder, eds., ACS Symposium Series No. 427, American Chemical Society, Washington. 1990: pp. 244-270.

S.D. Vidal, J.P. Simonin, and O. Bernard, *J. Phys. Chem.* 99, 6733 (1995).